International Journal of Robotics and Automation, Vol. 36, 2021

Special Issue: Automatic Detection and Assessment of Bridge Structures

STATIC MECHANICAL PROPERTIES EVOLUTION ANALYSIS OF A LONG-SPAN TRACK CABLE-STAYED BRIDGE

Xiaogang Li,* Peng Ding,* Xiaohu Chen,* Ling Xia,** and Shulin Tan*

Abstract

To analyse the static mechanical properties evolution law of long-span track cable-stayed bridges, an evaluation mode based on the parameter time-dependent effect change rate was proposed to evaluate a twin-tower and double-cable plane concrete cable-stayed bridge with a main span of 250 m. Finite element method (FEM) analysis was performed, considering the time-dependent change effect (including concrete shrinkage and creep, material strength, and cable elastic modulus) after 2 years of service since bridge completion. The results of the analysis were compared to the measured data detected by the structural health monitoring (SHM) system. The results show that the mechanical parameters of the long-span track cable-stayed bridge, including cable force, internal force of girder, deformation of girder, and displacement of main tower, constantly change with time and are stable with increasing service time. The FEM model can be modified using the measured parameters obtained from the SHM system, so the static mechanical evolution can be effectively predicted. The measured data can objectively describe the static mechanical properties evolution law based on the change rate index of the parameter time-dependent effect.

Key Words

Cable-stayed bridge, static mechanical properties, evolution, finite element, structural health monitoring

1. Introduction

With the development of urban rail transit, the application of long-span track bridges has become more widespread [1], [2]. The long-span track concrete cable-stayed bridge with the characteristics of beautiful structure, large span capacity, and strong adaptability, has become a widely popular bridge type. Compared to highway and railway bridges, track bridges are narrower with higher vibration and deformation requirements. They have the characteristics of large traffic volume, high operating frequency, strong load action, and marked structural response. They must meet strict requirements regarding bridge alignment and operational performance [3]. Hence, research of the evolution and control of their mechanical properties is in high demand.

The evolution of bridge mechanical properties is mainly related to the time-varying characteristics of materials, loads, and the natural environment. Researches have focused on the response and variation law of bridge structures under the action of various influencing factors. T. liu *et al.* [4] theoretically deduced the long-term deformation calculation formula of a fully prestressed concrete beam based on an effective modulus method. L. Chen *et al.* [5] studied the influence law of bridge panel shrinkage and creep on a combined beam cable-stayed bridge using finite element method (FEM) simulation. J. Z. Xin *et al.* [6] studied the behaviour of the bearing capacity evolution of corroded eccentric compression reinforced concrete columns. Studies have mostly used numerical analysis or model tests to analyse the long-term performance change rule, and few have been conducted on track cable-stayed bridges, or have employed evolutionary analysis based on real-time information [7]–[11]. Structural health monitoring (SHM) technology for automatic detection and assessment of existing and newly built long-span bridges has been widely developed [12], which provides emerging technologies for long-term performance research of long-span bridges.

In view of the particularities of track bridges and the paucity of researches, this article studies the evolution law of static mechanical properties of long-span track cable-stayed bridges. The Caijia Jialing River Bridge in China was taken as a case for analysis. Parameters of the cable, main girder, and main tower were analysed by FEM modelling in combination with real-time data collected by the SHM system [13]. Thus the static mechanical properties evolution law of large-span track bridges based on the parameter time-dependent effect change rate was obtained. This study can provide a reference for the service state and structural performance degradation analysis of long-span

* T. Y. Lin International Engineering Consulting (China) Co., Ltd, Chongqing 401121, China; e-mail: {li.xiaogang, dingpeng, chenxiaohu, tanshulin}@tylin.com.cn

** Traffic Construction Engineering Management Center of Luzhou City, Luzhou 646000, China; e-mail: 397972370@qq.com

Corresponding author: Peng Ding

Recommended by Dr. Jingzhou Xin

(DOI: 10.2316/J.2021.206-0534)

track bridges and lay a foundation for operational safety assessment.

2. Project Profile

The Caijia Jialing River Bridge is located between Jinshan Temple Station and Caojiawan Station in the Liangjiang New Area of Chongqing Municipality in China, adjoining the Lijia Group in the south and Caijia Group in the north, across the Jialing River.

It is a twin-tower and double-cable plane concrete cable-stayed bridge with tower-beam consolidation. The longitudinal span arrangement is $60 + 135 + 250 + 135 + 60$ m, and the transverse span arrangement is 1.5 m (cable zone) + 1.4 m (maintenance sidewalk) + 4.6 m (carriageway) + 4.6 m (carriageway) + 1.4 m (maintenance sidewalk) + 1.5 m (cable area). The main tower is diamond-shaped, while the auxiliary pier is hollow with a rectangular section. A total of 56 pairs of cables are used; these are made of steel strands with a standard strength of $f_{pk} = 1{,}860$ MPa, with a high-density polyethylene external sheath. The main girder is a concrete box girder with single-box–single-cell, with concrete strength grade C55. One segment is of 8 m long, and a cross-beam is arranged at the location of the stay cable, with cable anchorages at both ends of the cross-beam. The layout of the bridge is shown in Fig. 1.

The SHM system of the bridge was constructed. The subsequent static mechanical property evolution analysis was based on the data collected by the SHM system. The overall layout of sensor measuring point is shown in Fig. 2.

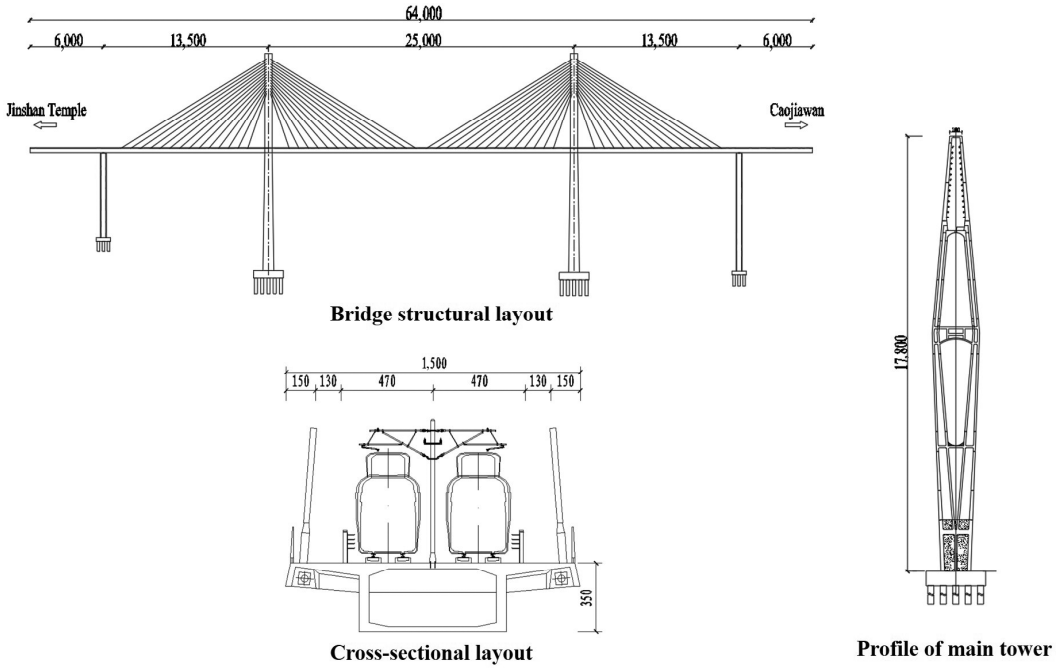

Figure 1. Caijia Jialing River Bridge layout (unit: cm).

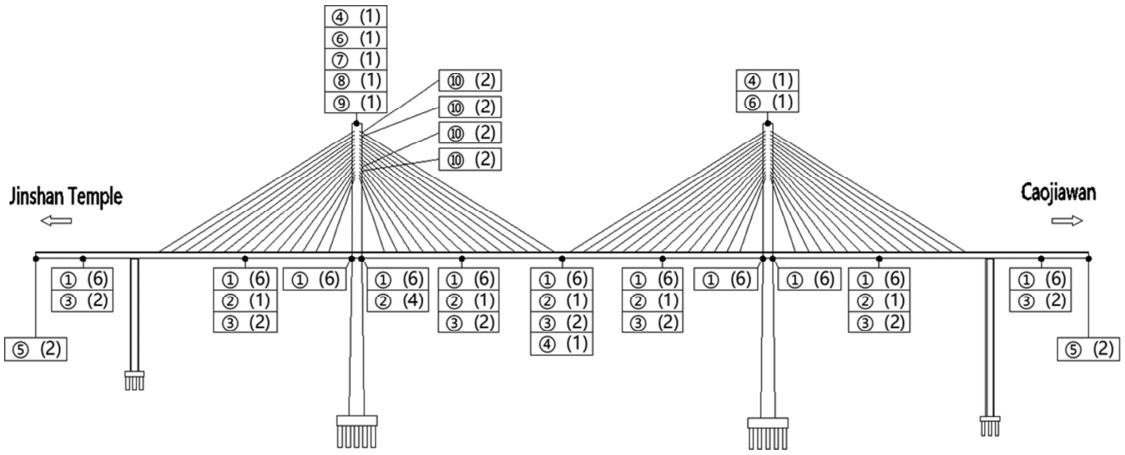

Figure 2. The overall layout of sensor measuring point: ① the stress sensor containing the temperature measurement function, ② the acceleration sensor, ③ the hydrostatic levelling, ④ Global Navigation Satellite System (GNSS), ⑤ the displacement meter, ⑥ the inclinometer, ⑦ the temperature and humidity sensor, ⑧ the pluviometer, ⑨ the dogvane and anemoscope and ⑩ the anchor cable meter. Also, the numbers in parentheses express the number of each sensor.

3. Static Mechanical Properties Influence Factor Analysis

The cable-stayed bridge is a kind of high-order statically indeterminate structure consisting of towers in compression, cables in tension, and girders in bending. The static mechanical properties include the cable force, main girder internal force and deformation, and main tower displacement. With the elapse of service time, the internal parameters of the structure will change, causing the change of such factors as structural forces, geometry, and boundaries, which further influence the change of structural mechanical static properties [14], [15].

3.1 Time-Dependent Effect of Concrete Shrinkage and Creep

Concrete shrinkage and creep has the characteristics of long duration, many influencing factors, and a complex process [16], [17], and it has a significant influence on the properties evolution of long-span track cable-stayed concrete bridges. According to *Specifications for Design of Highway Reinforced Concrete and Prestressed Concrete Bridges and Culverts* (JTG 3362-2018), the creep coefficient is calculated as

$$\varphi\left(t, t_0\right) = \varphi_0 \times \beta_c\left(t - t_0\right) \tag{1}$$

where t and t_0 are the respective concrete ages at the moments of calculating and loading, β_c is the coefficient of creep development with time, and φ_0 is the nominal creep coefficient expressed as

$$\varphi_0 = \varphi_{RH} \times \beta\left(f_{cm}\right) \times \beta\left(t_0\right) \tag{2}$$

where φ_{RH} is the coefficient associated with the annual average relative environmental humidity and component dimension, $\beta(f_{cm})$ is the coefficient associated with concrete strength grade, and $\beta(t_0)$ is the coefficient associated with loading age.

The shrinkage strain can be calculated by

$$\varepsilon_{cs}\left(t, t_s\right) = \varepsilon_{cso} \times \beta_s\left(t - t_s\right) \tag{3}$$

where t and t_s are the respective concrete ages of the moments of calculation and shrinkage commencement, β_s is the coefficient of creep development with time, and ε_{cso} is the nominal shrinkage coefficient expressed as

$$\varepsilon_{cso} = \varepsilon_s\left(f_{cm}\right) \times \beta_{RH} \tag{4}$$

where $\varepsilon_s\left(f_{cm}\right)$ is the coefficient associated with the concrete type and strength grade, and β_{RH} is the coefficient associated with annual average relative environmental humidity.

3.2 Time-Dependent Effect of Material Strength

The concrete compressive strength increase [18] is

$$f_c\left(t\right) = \beta_t \times f_c \tag{5}$$

with age effect coefficient as

$$\beta_t = e^{s\left(1-\sqrt{28/t}\right)} \geq 1 \tag{6}$$

where s varies by cement type and is 0.25 for ordinary and rapid hardening cement, $f_c(t)$ is concrete strength under monotonic static load at time t, and f_c is concrete strength under monotonic static load at the initial moment.

Concrete compressive strength increases slowly over time, and the limitation of compressive strength can be obtained as

$$y_r = \beta_t \times y_E \tag{7}$$

where y_r is the concrete time effect strength at initial loading time, β_t is the age effect coefficient at the moment of computation, and y_E is the concrete strength obtained from experimental results.

3.3 Time-Dependent Effect of Cable-Stayed Elastic Modulus

The change of elastic modulus of stay cables has the most significant influence on bridge static mechanical properties [19]. According to the *Guidelines for Design of Highway Cable-stayed Bridge* (JTG/T D65-01-2007), the cable's elastic modulus can be given as

$$E = \frac{E_0}{1 + \left(\gamma S \cos\alpha / 12\sigma^3\right)^2} \tag{8}$$

where E_0 is the elastic modulus of the stay cable, E is the conversion elastic modulus of the stay cable with the consideration of the sag effect, γ is the conversion volume–weight of the stay cable, S is the length of the stay cable, α is the dip angle of the stay cable and level, and σ is the stress in the stay cable.

4. Static Mechanical Properties Analysis

4.1 Finite Element Model

Midas/Civil was used to carry out a FEM analysis of the Caijia Jialing River Bridge. The model was divided into 819 nodes, 583 beam elements, and 112 truss elements, in which the main girder, pier, and main tower were simulated by a three-dimensional girder element, whereas the stay cables were truss elements. The model considered the combined actions of the stay cable, main girder, and main tower; complete consolidation between the main tower and pier bottom; rigid connection at boundaries between the main tower and stay cable, and between the main girder and stay cable; vertical, longitudinal, and transversal constraints arranged at the boundaries of auxiliary piers. In theoretical analysis, the load factors considered include live load, lateral swaying force, braking force, temperature load, wind load, and flow pressure of water. Also, the CEB-FIP (1990) model was used for shrinkage and creep of concrete. The refined model was established, as shown in Fig. 3.

4.2 Evolution Analysis

The static mechanical properties of a structure may undergo some changes with elapsed service time due to concrete contraction and creep, slack of stay cable, and other influences. The bridge had operated for 2 years since its completion. The evolution law was studied and explored by comparing the results of FEM analysis with the measured parameter data detected by the SHM system. A correction was made based on the principle of "null live load point" [20] to eliminate the temperature effect to the extent possible. Every 30 days as a cycle, the evolution law during 2 years of service since bridge completion was studied, with the parameter for evaluation being the static mechanical properties parameter time-dependent effect change rate:

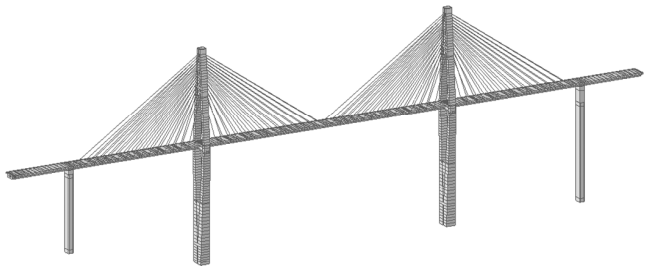

Figure 3. FEM model of the Caijia Jialing River Bridge.

$$c_{vr} = \frac{c_d - c_u}{c_u} \times 100\% \tag{9}$$

where c_{vr} is the time-dependent effect change rate of the static mechanical property parameter, c_d is the static mechanical properties parameter value after time-dependent effect, and c_u is the static mechanical properties parameter value at bridge completion.

4.2.1 Evolution Analysis of Stress of Stay Cables

Sensors were embedded during construction for cable force monitoring. Based on FEM analysis, the measured cable force and theoretical cable force were compared. Comparisons of the longest stay cable, X14, are shown in Table 1 and Fig. 4.

Table 1
Cable Force Change of the Longest Stay Cable, X14

Duration (day)	Theoretical Value (kN)	Theoretical Change Rate (%)	Measured Value (kN)	Measured Change Rate (%)	Difference of Value (kN)	Difference of Change Rate (%)
0	2,950.63	0.0	2,854.74	0.0	95.89	0.0
30	2,943.49	−0.2	2,844.46	−0.4	99.03	0.2
60	2,937.26	−0.5	2,846.10	−0.3	91.16	−0.2
90	2,932.22	−0.6	2,847.74	−0.3	84.48	−0.3
120	2,928.05	−0.8	2,815.65	−1.4	112.40	0.6
150	2,924.53	−0.9	2,819.45	−1.2	105.08	0.3
180	2,921.49	−1.0	2,827.13	−1.0	94.36	0.0
210	2,918.81	−1.1	2,829.66	−0.9	89.15	−0.2
240	2,916.40	−1.2	2,819.45	−1.2	96.95	0.0
270	2,914.20	−1.2	2,805.31	−1.7	108.89	0.5
300	2,912.17	−1.3	2,802.21	−1.8	109.96	0.5
330	2,910.27	−1.4	2,800.55	−1.9	109.72	0.5
360	2,908.47	−1.4	2,799.24	−1.9	109.23	0.5
390	2,906.77	−1.5	2,797.34	−2.0	109.43	0.5
420	2,905.14	−1.5	2,793.15	−2.2	111.99	0.7
450	2,903.58	−1.6	2,785.32	−2.4	118.26	0.8
480	2,902.08	−1.7	2,771.09	−2.9	130.99	1.2
510	2,900.62	−1.7	2,789.55	−2.3	111.07	0.6
540	2,899.22	−1.7	2,799.56	−1.9	99.66	0.2
570	2,897.86	−1.8	2,797.32	−2.0	100.54	0.2
600	2,896.54	−1.8	2,787.12	−2.4	109.42	0.6
630	2,895.26	−1.9	2,775.38	−2.8	119.88	0.9
660	2,894.01	−1.9	2,769.11	−3.0	124.90	1.1
690	2,892.80	−2.0	2,770.56	−3.0	122.24	1.0
720	2,891.62	−2.0	2,775.32	−2.8	116.30	0.8

Note: The initial value was found from construction monitoring. The sixth column is the difference between the theoretical and measured values. The last column is the difference between the theoretical and measured change rates.

The change of cable force tended to be stable with bridge service time. The overall trend of the measured stress and theoretical analysis was accordant, and the measured value was always smaller than the theoretical value with the maximum deviation of 130.99 kN. Furthermore, the difference between the theoretical and measured change rates was small; hence, the measured cable force could well reflect the mechanical properties and state of the stay cable in operation. The theoretical analysis could effectively predict the evolution of cable mechanical properties.

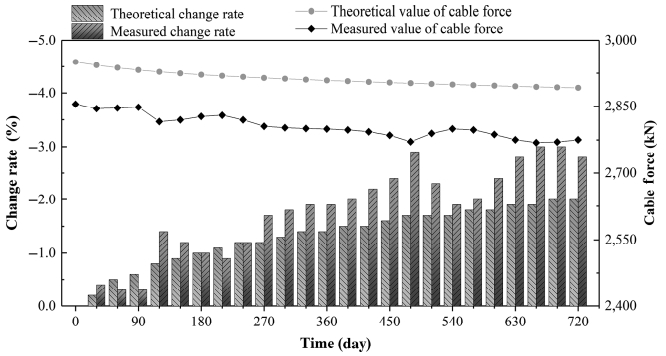

Figure 4. Cable force change of the longest stay cable, X14.

4.2.2 Main Girder Internal Force and Deformation Evolution Analysis

The stress sensors were deployed and applied during bridge construction. The embedded sensors were connected to the SHM system at the time of bridge completion, realized the "relay" (continuous monitoring) of stress monitoring of the main girder during the construction and operation. The main girder deformation was monitored by the GNSS, with the monitored data checked by a hydrostatic levelling system [21], [22]. Comparisons of the measured and theoretical values of stress and deformation at mid-span are shown in Tables 2 and 3, and Figs. 5 and 6.

Table 2
Main Girder Mid-Span Bottom Slab Stress Change

Duration (day)	Theoretical Value (MPa)	Theoretical Change Rate (%)	Measured Value (MPa)	Measured Change Rate (%)	Difference of Value (MPa)	Difference of Change Rate (%)
0	−10.20	0.0	−10.87	0.0	0.67	0.0
30	−10.00	−2.0	−10.52	−3.2	0.52	1.2
60	−9.86	−3.3	−10.31	−5.2	0.45	1.9
90	−9.75	−4.4	−10.21	−6.1	0.46	1.7
120	−9.65	−5.4	−10.35	−4.8	0.70	−0.6
150	−9.57	−6.2	−10.36	−4.7	0.79	−1.5
180	−9.50	−6.9	−10.18	−6.4	0.68	−0.5
210	−9.44	−7.5	−10.05	−7.5	0.61	0.0
240	−9.38	−8.0	−10.12	−6.9	0.74	−1.1
270	−9.32	−8.6	−10.15	−6.6	0.83	−2.0
300	−9.27	−9.1	−9.91	−8.8	0.64	−0.3
330	−9.23	−9.5	−9.65	−11.2	0.42	1.7
360	−9.18	−10.0	−9.44	−13.2	0.26	3.2
390	−9.14	−10.4	−9.31	−14.4	0.17	4.0
420	−9.10	−10.8	−9.37	−13.8	0.27	3.0
450	−9.06	−11.2	−9.55	−12.1	0.49	0.9
480	−9.02	−11.6	−9.67	−11.0	0.65	−0.6
510	−8.99	−11.9	−9.66	−11.1	0.67	−0.8
540	−8.95	−12.3	−9.53	−12.3	0.58	0.0
570	−8.92	−12.6	−9.36	−13.9	0.44	1.3
600	−8.89	−12.8	−9.24	−15.0	0.35	2.2
630	−8.85	−13.2	−9.41	−13.4	0.56	0.2
660	−8.82	−13.5	−9.51	−12.5	0.69	−1.0
690	−8.79	−13.8	−9.28	−14.6	0.49	0.8
720	−8.76	−14.1	−8.95	−17.7	0.19	3.6

Table 3
Main Girder Mid-Span Vertical Displacement Change

Duration (d)	Theoretical Value (mm)	Theoretical Change Rate (%)	Measured Value (mm)	Measured Change Rate (%)	Difference of Value (mm)	Difference of Change Rate (%)
0	−127	0.0	−127	0.0	0	0.0
30	−130	2.4	−130	2.4	0	0.0
60	−133	4.7	−134	5.5	1	−0.8
90	−135	6.3	−135	6.3	0	0.0
120	−138	8.7	−137	7.9	−1	0.8
150	−140	10.2	−144	13.4	4	−3.2
180	−143	12.6	−148	16.5	5	−3.9
210	−145	14.2	−149	17.3	4	−3.1
240	−147	15.7	−148	16.5	1	−0.8
270	−149	17.3	−147	15.7	−2	1.6
300	−151	18.9	−150	18.1	−1	0.8
330	−153	20.5	−155	22	2	−1.5
360	−154	21.3	−158	24.4	4	−3.1
390	−156	22.8	−160	26	4	−3.2
420	−157	23.6	−159	25.2	2	−1.6
450	−159	25.2	−157	23.6	−2	1.6
480	−160	26.0	−158	24.4	−2	1.6
510	−162	27.6	−162	27.6	0	0.0
540	−163	28.3	−168	32.3	5	−4.0
570	−165	29.9	−171	34.6	6	−4.7
600	−166	30.7	−171	34.6	5	−3.9
630	−168	32.3	−168	32.3	0	0.0
660	−169	33.1	−166	30.7	−3	2.4
690	−170	33.9	−167	31.5	−3	2.4
720	−171	34.6	−171	34.6	0	0.0

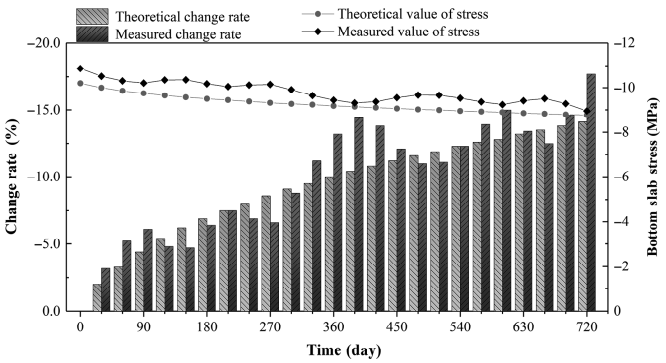

Figure 5. Main girder mid-span bottom slab stress change.

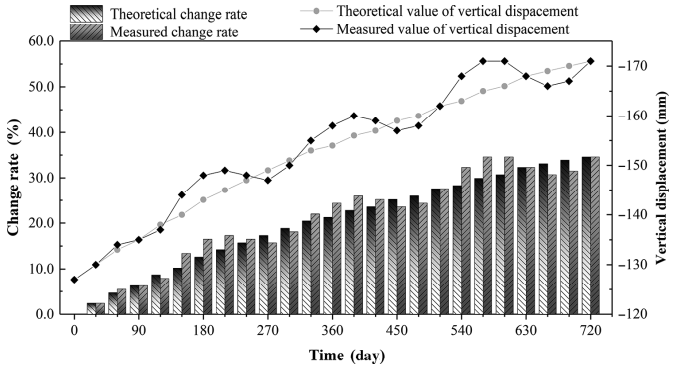

Figure 6. Vertical displacement change at mid-span of the main girder.

Table 4
South Tower Top Displacement Change

Duration (day)	Theoretical Value (mm)	Theoretical Change Rate (%)	Measured Value (mm)	Measured Change Rate (%)	Difference of Value (mm)	Difference of Change Rate (%)
0	−52	0.0	−52	0.0	0	0.0
30	−49	−5.8	−53	1.9	4	−7.7
60	−47	−9.6	−51	−1.9	4	−7.7
90	−45	−13.5	−41	−21.2	−4	7.7
120	−44	−15.4	−40	−23.1	−4	7.7
150	−42	−19.2	−41	−21.2	−1	2.0
180	−41	−21.2	−42	−19.2	1	−2.0
210	−39	−25.0	−42	−19.2	3	−5.8
240	−38	−26.9	−41	−21.2	3	−5.7
270	−37	−28.9	−39	−25.0	2	−3.9
300	−36	−30.8	−36	−30.8	0	0.0
330	−35	−32.7	−33	−36.5	−2	3.8
360	−34	−34.6	−31	−40.4	−3	5.8
390	−33	−36.5	−30	−42.3	−3	5.8
420	−32	−38.5	−31	−40.4	−1	1.9
450	−31	−40.4	−32	−38.5	1	−1.9
480	−30	−42.3	−32	−38.5	2	−3.8
510	−29	−44.2	−31	−40.4	2	−3.8
540	−28	−46.2	−29	−44.2	1	−2.0
570	−28	−46.2	−27	−48.1	−1	1.9
600	−27	−48.1	−25	−51.9	−2	3.8
630	−26	−50.0	−27	−48.1	1	−1.9
660	−25	−51.9	−27	−48.1	2	−3.8
690	−25	−51.9	−24	−53.9	−1	2.0
720	−24	−53.9	−23	−55.8	−1	1.9

Over the operation period of 2 years, the deviation of the measured stress time-dependent change rate from theory was relatively small. The measured value of vertical displacement at mid-span of the main girder agreed fairly well with its theoretical value. The maximum difference between the measured and theoretical values of bottom slab stress at the mid-span of the main girder was 0.83 MPa, and the maximum difference between the measured and theoretical values of vertical displacement at mid-span of the main girder was 6 mm. Both the measured values of bottom slab stress and vertical displacement were in the allowable range; thus, the main girder was in a normal state. The coincidence of theoretical and measured proved the accuracy of the FEM simulation analysis and the reliability of monitoring.

4.2.3 Main Tower Displacement Evolution Analysis

The main tower displacement was monitored by the GNSS and was checked by an inclinometer. The comparison of the measured value and the corresponding analysis result of the south tower displacement is shown in Table 4 and Fig. 7.

Within the operation period of 2 years, the maximum difference between the measured tower top displacement and corresponding theoretical analysis value was 4 mm, and the difference between the measured time-dependent effect change rate from theory was relatively small. No abnormality of the main tower was found. The measured data showed that with the growth of bridge service time, the main tower would deviate towards the centre of the

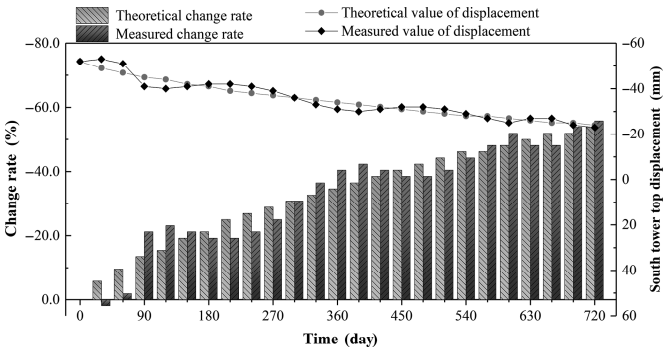

Figure 7. South tower top displacement change.

river. Therefore, in the construction stage of the main tower of such a structure, a rational pre-bias should be preset.

5. Conclusion

The change law of the static mechanical properties of long-span track cable-stayed bridges was studied based on a simulation analysis and the measured data of a SHM system. We provide the following concluding remarks.

1. During its operation period, a long-span track cable-stayed bridge might undergo a loss of cable force, progressive reduction of bottom slab compressive stress at mid-span of the main girder, continual downward deflection at mid-span, and main tower displacement toward the river centre. The change of mechanical parameters will gradually slow with bridge service time.
2. In the Caijia Jialing River Bridge, the measured static mechanical properties parameter data were generally close to the theoretical analysis. In addition, the differences of parameter time-dependent effect change rates were generally small, which indicated that the structure was in a normal state.
3. The FEM model could be modified by the measured parameter information detected by the SHM system. The accurate prediction of static mechanical properties evolution could be achieved through this method. The evaluation law could be objectively described with the time-dependent effect change rate index of the parameter.

Acknowledgement

This work was supported by Major Topic Special Key Research and Development Projects of the Artificial Intelligence Technology Innovation in Chongqing (cstc2017rgzn-zdyfX0029), the Technology Innovation and Application Demonstration Project of Chongqing (cstc2018jscx-mszdX0084).

References

[1] Editorial Department of *China Journal of Highway and Transport*, Review on China's bridge engineering research: 2014, *China Journal of Highway and Transport, 27*(05), 2014, 1–96.

[2] W.M. Zhai and C.F. Zhao, Frontiers and challenges of sciences and technologies in modern railway engineering, *Journal of Southwest Jiaotong University, 51*(2), 2016, 209–226.

[3] Q.H. Qin, Influence of linear change of urban rail transit bridge on train running behaviour, *Railway Engineering, 58*(07), 2018, 142–146.

[4] T. Liu, W.C. Xue, and W. Wang, Calculation on long-term deflections of fully prestressed concrete beams, *Engineering Mechanics, 33*(09), 2016, 116–122.

[5] L. Chen and C.Y Shao, Influential laws of concrete shrinkage and creep of composite girder cable-stayed bridge, *Bridge Construction, 45*(01), 2015, 74–78.

[6] J.Z. Xin, J.T. Zhou, Y.X. Zhou, *et al.*, Experimental study on bearing capacity evolution of reinforced concrete compression-bending members considering material deterioration, *Material Reports, 33*(14), 2019, 2362–2369.

[7] Y.B. Wang, P. Liao, Y. Jia, *et al.*, Effects of cyclic temperature on time-dependent deformation behaviour of long-span concrete arch bridge, *Bridge Construction, 49*(03), 2019, 57–62.

[8] M.Y. Liu, Q. Li, Y.B. Huang, *et al.*, Ultra-long-time performance of steel-concrete composite continuous beam in Hong Kong-Zhuhai-Macao Bridge with creep and shrinkage of concrete slabs, *China Journal of Highway and Transport, 29*(12), 2016, 60–69.

[9] J.T. Zhou, S.L. Tan, H. Tan, *et al.*, Research on structural improvement test in negative moment section with the change from simple supporting to continuous of the prestressed concrete T-beam, *Journal of China & Foreign Highway, 38*(04), 2018, 89–95.

[10] J.Z. Li, Z.W. Yu, and L. Song, Study on fatigue deflection and crack propagation laws of heavy-haul railway bridges, *China Civil Engineering Journal, 46*(09), 2013, 72–82.

[11] Z.S. Chen, C. Zhang, J.T. Zhou, *et al.*, Study of cable force of construction control and alignment control of main girders for long-span railway cable-stayed bridges, *Mathematical Models and Methods in Applied Sciences, 7*(9), 2013, 47.

[12] Z.S. Chen, X. Zhou, X. Wang, *et al.*, Deployment of a smart structural health monitoring system for long-span arch bridges: A review and a case study, *Sensors, 17*(9), 2017, 2151.

[13] J.T. Zhou, Y. Chen, X.G. Li, *et al.*, A new safety evaluation method for long-span bridges with tele-monitoring systems, *Intelligent Automation & Soft Computing, 16*(5), 2010, 635–644.

[14] O. Yang, H. Li, and J.P. Ou, Life-cycle evolution of the ultimate load carrying capacity of RC cable-stayed bridges, *China Civil Engineering Journal, 45*(03), 2012, 116–126.

[15] S.J. Chen, S.H. Tang, G.G. Zhang, *et al.*, Experiment on long-term performance of concrete cable-stayed bridge, *China Journal of Highway and Transport, 24*(04), 2011, 39–49.

[16] J.S. Fan, J.G. Nie, and H. Wang, Long-term behavior of composite beams with shrinkage, creep and cracking (I): experiment and calculation, *China Civil Engineering Journal, 42*(03), 2009, 8–15.

[17] J.F. Yu, Y.K. Wu, and X. Su, Study on predication of line optimization of large-span concrete cable-stayed bridges, *Journal of Railway Science and Engineering, 15*(01), 2018, 133–140.

[18] W.J. Yang and Y. Wang, Diachronic change model of compressive strength and elastic modulus of concrete at early age, *Journal of China & Foreign Highway, 27*(6), 2007, 149–152.

[19] Y.L. Ding, Y. Bian, H.W. Zhao, *et al.*, Long-term monitoring and analysis of vertical deflections of a highway-railway cable-stayed bridge under operation conditions, *Journal of Railway Science and Engineering, 14*(02), 2017, 271–277.

[20] H.J. Wu, Y. Wei, Y.B. Huang, *et al.*, Null live load point identification method of continuous rigid bridges based on monitoring data, *Journal of Chongqing Jiaotong University (Natural Science), 32*(S1), 2013, 884–887.

[21] X.G. Li, D. Hui, J.T. Zhou, *et al.*, Large span cable-stayed bridge health monitoring and evaluation system building and application, *Journal of China & Foreign Highway, 36*(2), 2016, 92–97.

[22] J.T. Zhou, X.G. Li, R.C. Xia, *et al.*, Health monitoring and evaluation of long-span bridges based on sensing and data analysis: A survey, *Sensors, 17*(3), 2017, 603.

Biographies

Xiaogang Li received his PhD in Bridge Engineering from Chongqing Jiaotong University, China. Currently, he is an Engineer in T.Y. Lin International Engineering Consulting (China) Co., Ltd, Chongqing, China. His current research interests include bridge health monitoring, safety assessment, and strengthening.

Peng Ding received his master degree in Bridge Engineering from Chongqing Jiaotong University, China. Currently, he is an Engineer in T.Y. Lin International Engineering Consulting (China) Co., Ltd, Chongqing, China. His current research interests include bridge health monitoring, safety assessment, and strengthening.

Xiaohu Chen received his PhD in Civil Engineering from University of Maryland, College Park, Maryland USA. He is now an Engineer in T.Y. Lin International Engineering Consulting (China) Co., Ltd, Chongqing, China. His current research interests include bridge design and health monitoring.

Ling Xia received his master degree in Civil Engineering. He is now an Engineer in Traffic Construction Engineering Management Center of Luzhou City, Luzhou, China. His current research interests include bridge and tunnel engineering.

Shulin Tan received his master degree in Bridge Engineering from Chongqing Jiaotong University, Chongqing, China. Currently, he is an Engineer in T.Y. Lin International Engineering Consulting (China) Co., Ltd, Chongqing, China. His current research interests include bridge health monitoring, safety assessment, and strengthening.